in vivo *37*: 519-523 (2023)
doi:10.21873/invivo.13109

Near-infrared Fluorescence Imaging for Detecting Pancreatic Liver Metastasis in an Orthotopic Athymic Mouse Model

LUCAS D. LEE[1,2], NINA A. HERING[1], MIRIAM ZIBELL[1], LEONARD A. LOBBES[1], CARSTEN KAMPHUES[1,2], JOHANNES C. LAUSCHER[1], GEORGIOS A. MARGONIS[3], HENDRIK SEELIGER[4], KATHARINA BEYER[1], BENJAMIN WEIXLER[1] and IOANNIS POZIOS[1]

[1]*Department of General and Visceral Surgery, Charité – Universitätsmedizin Berlin, Corporate Member of Freie Universität Berlin and Humboldt-Universität zu Berlin, Berlin, Germany;*
[2]*Department of General, Visceral and Minimally Invasive Surgery, Park Klinik Weissensee, Berlin, Germany;*
[3]*Department of Surgery, Memorial Sloan Kettering Cancer Center, New York City, NY, U.S.A.;*
[4]*IU Health University, Mainz, Germany*

Abstract. *Background/Aim: Evidence of metastatic disease precludes oncological resection of pancreatic cancer. Near-infrared (NIR) fluorescent labels, such as indocyanine green (ICG), assist in the intraoperative detection of occult and micrometastatic liver disease. The present study aimed to analyse the role of NIR fluorescence imaging using ICG for pancreatic liver disease as proof of concept in an orthotopic athymic mouse model. Materials and Methods: Pancreatic ductal adenocarcinoma was induced by injecting L3.6pl human pancreatic tumour cells into the pancreatic tail of seven athymic mice. After four weeks of tumour growth, ICG was injected into the tail vein and NIR fluorescence imaging was performed at harvest to determine tumour-to-liver ratios (TLR) using Quest Spectrum® Fluorescence Imaging Platform. Results: Pancreatic tumour growth and liver metastasis could be visually confirmed for all seven animals. None of the hepatic metastases showed any detectable ICG-uptake. ICG-staining failed to visualize the liver metastases or to increase fluorescence intensity of the rim around the hepatic lesions. Conclusion: ICG-staining fails to visualize liver metastases induced by L3.6pl pancreatic tumour cells in athymic nude mice by NIR fluorescence imaging. Further studies are necessary to delineate the underlying mechanism for insufficient ICG uptake in these pancreatic liver metastases and for the lack of a fluorescent rim around the liver lesions.*

Correspondence to: Ioannis Pozios, MD, Department of General and Visceral Surgery, Campus Benjamin Franklin, Charité – Universitaetsmedizin Berlin, Hindenburgdamm 30, 12203 Berlin, Germany. Tel: +49 30450522702, e-mail: ioannis.pozios@charite.de

Key Words: Near-infrared (NIR) fluorescence imaging, indocyanine green (ICG), TLR, pancreatic cancer, liver metastasis, athymic mouse model.

Despite modern multimodality treatment, pancreatic ductal adenocarcinoma (PDAC) continues to be the seventh leading cause for cancer-related deaths worldwide with a poor 5-year survival rate of 9% (1, 2). Surgical resection remains the only mainstay of curative-intent treatment, given the absence of distant metastasis at diagnosis, which accounts for only 20% of the patients (2). However, up to 20% of resectable PDACs, based on preoperative computed tomography (CT) scans, undergo surgical abort due to intraoperative evidence of metastatic disease (3).

In comparison to CT, magnetic resonance imaging (MRI) has been shown to achieve higher sensitivity (85% vs. 75%) for the detection of liver tumours (4). While the current National Comprehensive Cancer Network (NCCN) guidelines primarily recommend liver MRI to further delineate unclear findings in prior CT, the German guidelines have recently incorporated MRI as standard staging method to rule out liver disease (5, 6). Still, occult and microscopic liver tumours frequently remain unseen in high resolution imaging. These patients do fare worse than others after curative resection. Presently, near-infrared (NIR) fluorescence imaging using indocyanine green (ICG) is successfully applied to detect colorectal liver metastasis not only in experimental studies *in vivo* (7), but it is a well-established method in oncologic surgery enabling better staging and more complete surgical resection with a potential prognostic benefit for the patients (8, 9). We hypothesize that this technique may also help to close the diagnostic gap for pancreatic liver tumours. ICG accumulates in the tumour tissue. It ideally emits near-infrared fluorescence between

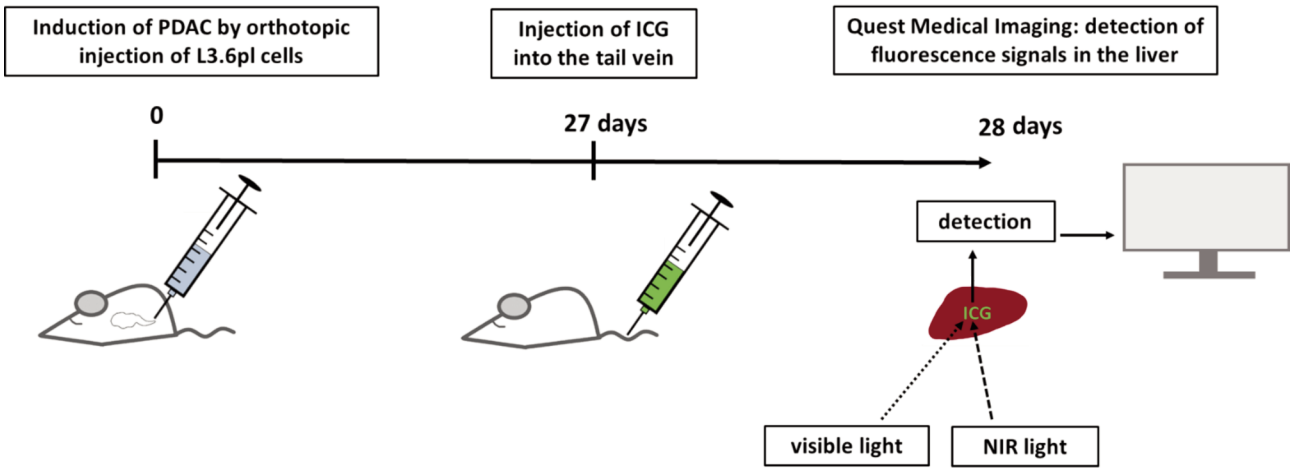

Figure 1. *Experimental schema. Pancreatic ductal adenocarcinoma (PDAC) was induced by orthotopic injection of L3.6pl cells into the pancreatic tail. Twenty-seven days later, indocyanine green (ICG) was injected into the tail vein. After 24 h, mice were sacrificed and Quest Spectrum® Fluorescence Imaging was performed for metastasis imaging.*

700 and 900 nm and is cleared by the liver through bile excretion without any mentionable adverse effects (10). Both the Food and Drug Administration (FDA) and European Medicines Agency (EMA) have approved ICG for clinical use (10).

Few studies so far have addressed the question whether image guided surgery with intraoperative ICG-staining may also be used to detect liver metastasis derived from PDAC. Therefore, the aim of this current study was to explore as proof of concept the potential of intraoperative ICG-staining to reliably visualize pancreatic liver tumours using an orthotopic mouse model of PDAC.

Materials and Methods

Cell lines and reagents. L3.6pl is a secondary highly metastatic human pancreatic adenocarcinoma cell line derived from an orthotopic mouse xenograft model (1). Cells were maintained in Dulbecco's Minimal Essential Medium (Invitrogen GmbH, Karlsruhe, Germany), supplemented with 10% fetal bovine serum and 1% penicillin streptomycin (Thermo Fisher Scientific, Darmstadt, Germany), and were cultured in a humidified atmosphere of 5% CO_2 at 37˚C.

Induction of PDAC and administration of ICG in vivo. Male, 6-week-old Balb/c nu/nu mice were purchased from Janvier (Le Genest-Saint, France). Animals were housed at 22±2˚C with a 12-h light/dark cycle under specific pathogen-free conditions. Anaesthesia and operative procedure were performed as described previously (11-13). After laparotomy and pancreas mobilization, 10^6 L3.6pl cells were injected into the pancreatic tail of seven animals. Animals were sacrificed 28 days post orthotopic tumour induction. All animals were inspected for primary tumour growth and metastatic liver disease. Twenty-four hours prior to animal sacrifice and subsequent median laparotomy for liver procurement, 0.025 mg ICG (VerDye, Diagnostic Green GmbH, Aschheim Germany, 25 mg vials) was administered *via* tail vein injection (ICG concentration 0.25 mg/ml). An experimental scheme is given in Figure 1. Animal care and manipulation were in agreement with the European Union Guidelines on Animal Experiments. All animal experiments were approved by the regional authority (Landesamt für Gesundheit und Soziales, Berlin, G0212/17), and performed in compliance with the European Union guideline 2010/63/EU.

Table I. *Tumour-to-liver ratio (TLR) based on fluorescence density of healthy liver parenchyma and respective liver metastasis as measured by ImageJ Software.*

Mouse	TLR
1	1.09
2	0.98
3	0.78
4	0.87
5	1.0
6	1.15

Tumour-to-liver ratio (TLR). Quest Spectrum® Fluorescence Imaging Platform (Quest Medical Imaging, Middenmeer, the Netherlands) was used at animal harvest to assess tumour fluorescence. ImageJ Software was used to determine the fluorescence densities of healthy liver parenchyma, liver metastasis, and gallbladder as a positive control. Then, TLR fluorescence signal was calculated for each mouse by dividing maximum tumour fluorescence by maximum liver fluorescence. Mean TLR was calculated using SPSS version 28 (IBM, Armonk, NY, USA).

Results

All animals showed primary tumour growth. One animal had to be prematurely sacrificed and excluded from analysis due

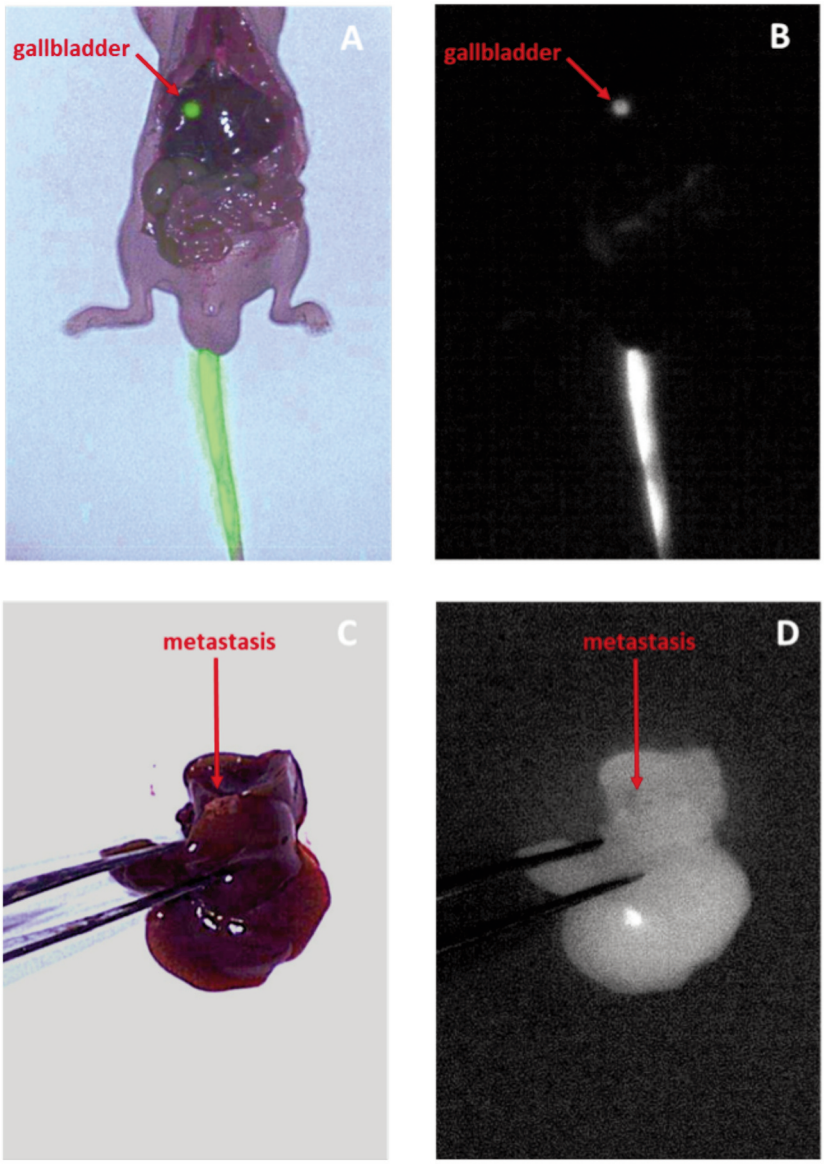

Figure 2. *Indocyanine green (ICG) fluorescence detection of pancreatic liver metastasis in nude mice. (A) Visual identification of ICG accumulation in the gallbladder and (B) corresponding ICG-visualization using Quest Spectrum® Fluorescence Imaging Platform. (C) Visual identification of liver metastasis and (D) corresponding Quest Spectrum® Fluorescence Imaging Platform.*

to tumour cachexia. Accumulation of ICG in the gallbladder served as a positive control of successful ICG application (Figure 2A and B). The liver was extracted at animal sacrifice and tumour metastases were visually confirmed (Figure 2C). Quest Medical Imaging System was then used to detect ICG-staining of the liver tumours (Figure 2D). All the remaining six animals clearly developed tumour growth in the liver, but none were detectable with ICG-staining. For quantification, TLR was calculated (Table I). The mean TLR was 0.83±0.38 (n=6). Liver tumours in mouse no. 3 and 4 even showed less density compared to healthy liver parenchyma, *i.e.*, TLR <1 (Table I).

Discussion

This study was designed as proof of concept to demonstrate that real-time ICG-staining reliably visualizes pancreatic liver tumours in an orthotopic athymic mouse model. However, our data clearly reveal that ICG did not stain pancreatic cancer metastasis in this model.

Tashiro *et al*. were already able to successfully stain colorectal liver metastases in athymic nude mice with ICG and concluded that this would further help to improve the detection of occult metastases in a preclinical setting (7).

In another Japanese study, ICG-staining was clinically explored for intraoperative detection of pancreatic liver tumours. Indeed, thirteen out of 49 patients (26.5%) had abnormal ICG-findings in the liver with subsequent frozen-section analyses that confirmed metastatic disease in nearly two-thirds of the patients (14). Another independent Japanese study reported similar results with 24% of the PDAC patients showing abnormal ICG-staining in the liver at surgical exploration and nearly two-thirds showing positive pathology for metastatic disease (15). Based on these studies, intraoperative ICG-staining could potentially help to avoid complex resection in up to 26.5% of patients, who were initially staged as resectable. Shirakawa *et al*. are conducting an ongoing prospective trial to investigate NIR-technology with ICG during staging laparoscopy for borderline resectable PDAC (16). The results are pending and much anticipated.

In our study, all animals developed large PDAC liver metastases (Figure 2A). However, none showed any detectable ICG-uptake or increased fluorescence intensity of the rim around the liver metastases (Figure 2B). The corresponding TLR values (Table I) confirm the lack of relevant ICG-uptake in the evident liver tumours. Our findings suggest that liver tumours stemming from the L3.6pl cell line show low ICG-avidity. The biomolecular underpinnings are unclear. However, specific PDAC cell lines with distinct molecular signatures may infer differential carcinogenesis and therefore also differential intracellular mechanisms that may explain differences in ICG-avidity. Recent data support the oncological significance of molecular subtypes of PDAC as they appear to correlate with clinical outcome (17).

A previous study using fluorescence imaging to detect colorectal liver metastasis in oncologic surgical patients showed that all fluorescent liver metastases presented a fluorescent rim around the tumour, but no increase in the fluorescent signal of the tumour tissue was described (9). In detail, fluorescence microscopy showed that the fluorescent rim in liver tissue appears in the transition zone between tumour and normal liver tissue. The intracellular accumulation of ICG was observed in and around immature hepatocytes directly surrounding the tumour, and being compressed by it (9). The architecture of the hepatic parenchyma is often transformed by the liver metastases leading to parenchyma compression, inflammation, ductular transformation, and increased presence of immature hepatocytes (18), which frequently have reduced expression of organic anion transporters, including ICG transporter, showing an impaired biliary clearance (19–22). Analog to liver metastases, this increased fluorescence signal would also be expected around the hepatic PDAC lesions. However, this could not be confirmed in our study, as no relevant ICG-uptake could be visualized in any of the rims surrounding the liver metastases (Figure 2B). The small size of the liver metastases in our mouse model may be an explanation for this difference and further investigation using fluorescence microscopy may contribute to understand the lack of a clear fluorescent ring around these PDAC hepatic metastases.

In summary, PDAC induction by L3.6pl cells in orthotopic athymic nude mice is not an adequate model to investigate NIR fluorescence imaging with ICG for pancreatic liver disease in a preclinical setting. However, other studies have shown a detection rate of about 26% for occult liver disease in pancreatic cancer, which should not be dismissed. Instead, further studies using fluorescence microscopy are needed to understand the lack of ICG-uptake in the liver tissue surrounding the PDAC metastases from different PDAC cell lines and is necessary to compare these data with human liver tissue from patients with metastatic PDAC.

Conflicts of Interest

The Authors declare no conflicts of interest in relation to this study.

Authors' Contributions

IP designed this experiment. NAH, MZ, and IP conducted experiments. LDL and IP analysed data. LAL, BW, and IP explained the experimental results. NAH and MZ prepared these figures. LDL, NAH, and IP wrote the manuscript. NAH, JCL, and BW contributed to manuscript editing. CK, JCL, GAM, HS, and KB revised the manuscript. All Authors participated in reading and discussing the manuscript.

Acknowledgements

The Authors thank Marco Arndt for the excellent technical assistance and Carolin Oberbeck for the animal care.

References

1 Bray F, Ferlay J, Soerjomataram I, Siegel RL, Torre LA and Jemal A: Global cancer statistics 2018: GLOBOCAN estimates of incidence and mortality worldwide for 36 cancers in 185 countries. CA Cancer J Clin *68(6)*: 394-424, 2018. PMID: 30207593. DOI: 10.3322/caac.21492

2 van Roessel S, van Veldhuisen E, Klompmaker S, Janssen QP, Abu Hilal M, Alseidi A, Balduzzi A, Balzano G, Bassi C, Berrevoet F, Bonds M, Busch OR, Butturini G, Del Chiaro M, Conlon KC, Falconi M, Frigerio I, Fusai GK, Gagnière J, Griffin O, Hackert T, Halimi A, Klaiber U, Labori KJ, Malleo G, Marino MV, Mortensen MB, Nikov A, Lesurtel M, Keck T, Kleeff J, Pandé R, Pfeiffer P, Pietrasz D, Roberts KJ, Sa Cunha A, Salvia R, Strobel O, Tarvainen T, Bossuyt PM, van Laarhoven HWM, Wilmink JW, Groot Koerkamp B, Besselink MG and European-African Hepato-Pancreato-Biliary Association: Evaluation of adjuvant chemotherapy

in patients with resected pancreatic cancer after neoadjuvant FOLFIRINOX treatment. JAMA Oncol *6(11)*: 1733-1740, 2020. PMID: 32910170. DOI: 10.1001/jamaoncol.2020.3537

3 Somers I and Bipat S: Contrast-enhanced CT in determining resectability in patients with pancreatic carcinoma: a meta-analysis of the positive predictive values of CT. Eur Radiol *27(8)*: 3408-3435, 2017. PMID: 28093626. DOI: 10.1007/s00330-016-4708-5

4 Hong SB, Choi SH, Kim KW, Kim SY, Kim JH, Kim S and Lee NK: Meta-analysis of MRI for the diagnosis of liver metastasis in patients with pancreatic adenocarcinoma. J Magn Reson Imaging *51(6)*: 1737-1744, 2020. PMID: 31664776. DOI: 10.1002/jmri.26969

5 NCCN Clinical Practice Guidelines in Oncology for Pancreatic Adenocarcinoma. Available at: https://www.nccn.org/professionals/physician_gls/pdf/pancreatic_blocks.pdf [Last accessed on June 26, 2022]

6 Schmidt T: [S3 guideline "Exocrine Pancreatic Cancer"]. Chirurgie (Heidelb) *93(10)*: 1006, 2022. PMID: 36163276. DOI: 10.1007/s00104-022-01689-6

7 Tashiro Y, Hollandsworth HM, Nishino H, Yamamoto J, Amirfakhri S, Filemoni F, Sugisawa N, Aoki T, Murakami M, Hoffman RM and Bouvet M: Indocyanine green labels an orthotopic nude-mouse model of very-early colon-cancer liver metastases. In Vivo *34(5)*: 2277-2280, 2020. PMID: 32871750. DOI: 10.21873/invivo.12038

8 Liberale G, Bourgeois P, Larsimont D, Moreau M, Donckier V and Ishizawa T: Indocyanine green fluorescence-guided surgery after IV injection in metastatic colorectal cancer: A systematic review. Eur J Surg Oncol *43(9)*: 1656-1667, 2017. PMID: 28579357. DOI: 10.1016/j.ejso.2017.04.015

9 van der Vorst JR, Schaafsma BE, Hutteman M, Verbeek FP, Liefers GJ, Hartgrink HH, Smit VT, Löwik CW, van de Velde CJ, Frangioni JV and Vahrmeijer AL: Near-infrared fluorescence-guided resection of colorectal liver metastases. Cancer *119(18)*: 3411-3418, 2013. PMID: 23794086. DOI: 10.1002/cncr.28203

10 Verbeek FP, van der Vorst JR, Schaafsma BE, Hutteman M, Bonsing BA, van Leeuwen FW, Frangioni JV, van de Velde CJ, Swijnenburg RJ and Vahrmeijer AL: Image-guided hepatopancreatobiliary surgery using near-infrared fluorescent light. J Hepatobiliary Pancreat Sci *19(6)*: 626-637, 2012. PMID: 22790312. DOI: 10.1007/s00534-012-0534-6

11 Bruns CJ, Harbison MT, Kuniyasu H, Eue I and Fidler IJ: In vivo selection and characterization of metastatic variants from human pancreatic adenocarcinoma by using orthotopic implantation in nude mice. Neoplasia *1(1)*: 50-62, 1999. PMID: 10935470. DOI: 10.1038/sj.neo.7900005

12 Nawrocki ST, Bruns CJ, Harbison MT, Bold RJ, Gotsch BS, Abbruzzese JL, Elliott P, Adams J and McConkey DJ: Effects of the proteasome inhibitor PS-341 on apoptosis and angiogenesis in orthotopic human pancreatic tumor xenografts. Mol Cancer Ther *1(14)*: 1243-1253, 2002. PMID: 12516957.

13 Pozios I, Seel NN, Hering NA, Hartmann L, Liu V, Camaj P, Müller MH, Lee LD, Bruns CJ, Kreis ME and Seeliger H: Raloxifene inhibits pancreatic adenocarcinoma growth by interfering with ERβ and IL-6/gp130/STAT3 signaling. Cell Oncol (Dordr) *44(1)*: 167-177, 2021. PMID: 32940862. DOI: 10.1007/s13402-020-00559-9

14 Yokoyama N, Otani T, Hashidate H, Maeda C, Katada T, Sudo N, Manabe S, Ikeno Y, Toyoda A and Katayanagi N: Real-time detection of hepatic micrometastases from pancreatic cancer by intraoperative fluorescence imaging: preliminary results of a prospective study. Cancer *118(11)*: 2813-2819, 2012. PMID: 21990070. DOI: 10.1002/cncr.26594

15 Katada T, Hashidate H, Yokoyama N, Sudo N, Mitsuma K and Otani T: Initial features of hepatic metastases from pancreatic cancer: Histological and radiolographical appraisal of hepatic micrometastases detected by real-time fluorescent imaging. Pancreas *46(9)*: 1196-1201, 2017. PMID: 28902791. DOI: 10.1097/MPA.0000000000000915

16 Shirakawa S, Toyama H, Kido M and Fukumoto T: A prospective single-center protocol for using near-infrared fluorescence imaging with indocyanine green during staging laparoscopy to detect small metastasis from pancreatic cancer. BMC Surg *19(1)*: 165, 2019. PMID: 31699083. DOI: 10.1186/s12893-019-0635-0

17 N Kalimuthu S, Wilson GW, Grant RC, Seto M, O'Kane G, Vajpeyi R, Notta F, Gallinger S and Chetty R: Morphological classification of pancreatic ductal adenocarcinoma that predicts molecular subtypes and correlates with clinical outcome. Gut *69(2)*: 317-328, 2020. PMID: 31201285. DOI: 10.1136/gutjnl-2019-318217

18 Vermeulen PB, Colpaert C, Salgado R, Royers R, Hellemans H, Van Den Heuvel E, Goovaerts G, Dirix LY and Van Marck E: Liver metastases from colorectal adenocarcinomas grow in three patterns with different angiogenesis and desmoplasia. J Pathol *195(3)*: 336-342, 2001. PMID: 11673831. DOI: 10.1002/path.966

19 Oshima H, Kon J, Ooe H, Hirata K and Mitaka T: Functional expression of organic anion transporters in hepatic organoids reconstructed by rat small hepatocytes. J Cell Biochem *104(1)*: 68-81, 2008. PMID: 18022823. DOI: 10.1002/jcb.21601

20 de Graaf W, Häusler S, Heger M, van Ginhoven TM, van Cappellen G, Bennink RJ, Kullak-Ublick GA, Hesselmann R, van Gulik TM and Stieger B: Transporters involved in the hepatic uptake of (99m)Tc-mebrofenin and indocyanine green. J Hepatol *54(4)*: 738-745, 2011. PMID: 21163547. DOI: 10.1016/j.jhep.2010.07.047

21 Cui Y, König J, Leier I, Buchholz U and Keppler D: Hepatic uptake of bilirubin and its conjugates by the human organic anion transporter SLC21A6. J Biol Chem *276(13)*: 9626-9630, 2001. PMID: 11134001. DOI: 10.1074/jbc.M004968200

22 Ros JE, Roskams TA, Geuken M, Havinga R, Splinter PL, Petersen BE, LaRusso NF, van der Kolk DM, Kuipers F, Faber KN, Müller M and Jansen PL: ATP binding cassette transporter gene expression in rat liver progenitor cells. Gut *52(7)*: 1060-1067, 2003. PMID: 12801967. DOI: 10.1136/gut.52.7.1060

Received January 5, 2023
Revised January 15, 2023
Accepted January 16, 2023